Imperial Journal of Interdisciplinary Research (IJIR)
Vol-3, Issue-6, 2017
ISSN: 2454-1362, http://www.onlinejournal.in

Study of Field Emission Characteristics of Carbon Nanotube Films in an Indigenously Developed Field Emission Set Up

P. Girdhar, S. Ghosh and V. D. Vankar
Nanostech Laboratory, Indian Institute of Technology Delhi, Hauz Khas, New Delhi-110016

Abstract: *We report here field emission (FE) properties of carbon nanotube (CNT) films grown by microwave plasma enhanced chemical vapor deposition (MPECVD) technique on catalyst (iron) coated Si substrate. FE measurements were carried out in a high vacuum compatible field emission set up designed and fabricated indigenously. The set up is made in diode configuration, with a precision control of electrodes separation (down to 5 μm) and tested up to a pressure of 5 × 10^{-7} torr with the help of a rotary and turbo molecular pump (TMP). The role of microstructure of the films on their FE properties has been investigated. Growth of the films on a patterned substrate was also carried out and their FE characteristics have been reported.*

1. Introduction

Due to the complex hybridization possibilities (i.e. sp^3 and sp^2) of carbon, different structures of carbon are found in nature including diamond, graphite, fullerene etc. Rolling of graphite sheets results in formation of carbon nanotubes (CNTs), which can be formed as single wall CNT (SWCNT) or multi wall CNT (MWCNT). Since their discovery in 1991 [1], there have been increasing interests in CNTs due to its unique structure and properties including high Young's modulus (of the order of 1.1 to 1.3 TPa for MWNTs [2]), high thermal conductivity (~ 3000 W/ milli Kelvin [3]), and chemical inertness. These have a wide variety of applications in the fields of electronics, hydrogen storage, medical sciences etc. [4].

Over the years, several methods have been developed to produce CNTs of different structure. However, the three mainly used methods are: arc-discharge [5-6], laser ablation [7] and chemical vapor deposition (CVD) [8]. In this work, Microwave Plasma Enhanced CVD (MPECVD) has been used for the growth of CNT films. MPECVD is one of the variants of CVD in which CNT growth can be accomplished at relatively lower substrate temperatures (~ 500-700^0 C) due to the presence of active plasma species. Further, the controllability of process parameters and alignment of CNTs is better as compared to conventional CVD.

Field Emission i.e. the electric field induced emission of electrons from a solid, is one of the most studied properties of CNTs. The structure of CNT, comprising of a long, thin cylinder terminated in a hemispherical cap, results in one of the highest attainable surface fields at its tip. Due to their high aspect ratio, mechanical strength, chemical inertness and long lifetime, CNTs are found to be excellent field emitters [9-10]. A CNT field emission device can be made by applying a voltage between two electrodes, one of which is coated with an array of nanotubes. CNT electron sources have a variety of applications including flat panel displays [11-14], X-ray tube sources [15], CNT based lamps and in nanoprobes and sensors [4]. CNT based field emission sources have low threshold fields (of the order of 1-3 V/μm) and high current densities (of the order of 10 mA/cm^2). Moreover, these sources have much higher brightness (~ 30 times), higher chemical and thermal stability, low voltage operation and very small energy spread as compared to conventional electron sources.

The field emission properties of CNT films are strongly dependent on the structure, density and morphology of the film, which in turn can be controlled by varying the parameters (like pressure, gas flow ratio, microwave power and time of deposition) of the MPECVD process [16-17]. For emission from CNT film to be maximum, the intertube distance should be twice the height of the CNTs. Emission from low density CNT films is poor because there are few emitting sites of insufficient β factor, and emission from densely packed CNT films is poor because of reductions in the field enhancement factor due to screening effects [18]. One of the methods of reducing the screening effect is to pattern the catalyst film before CNT growth. In the present work, CNT growth has been carried out on a square pattern (of

size 10 μm x 10 μm) of Fe pads with inter separation of 10 μm. The role of microstructure on field emission properties is also investigated

2. Experimental Details

2.1. Design of Field Emission set-up

A highly polished stainless steel high vacuum chamber was fabricated having following dimensions:
(a) External diameter ~ 34 cm
(b) Internal diameter ~ 29 cm
(c) Height ~ 23.5 cm

The chamber has a cylindrical geometry with several ports. These ports are basically constructed to connect pirani and penning gauge heads with controllers. Turbomolecular pump, backed by rotary pump is connected in one port through a high vacuum gate valve. Additional ports for feed-throughs for making electrical connections and a viewing window for monitoring are also present. Inside the chamber, there is arrangement for having the cathode and anode plate insulated from each other. Figure 1 and 2 show the front view and top view of the field emission setup. The anode is a highly polished stainless steel plate having a diameter of 19 cm. The movement of the cathode can be digitally controlled by using a controller to the accuracy of 5 μm, which in turn gives the adjustable distance between the cathode and anode. Figure 3 shows the cathode movement assembly with the digital controller. During the initial phase of integration, the chamber was connected to a rotary pump (DS 102 of Varian make) to check for the vacuum compatibility. A vacuum of the order of 10^{-3} torr was obtained. The pressure was measured by digital Pirani gauge (model no PHG-11 of Vactech). Subsequently a turbo pump (TV-301 Navigator of Varian) with turbo controller (Turbo-V 301 of Varian) was integrated to the chamber through a separate port, with the help of which a vacuum of the order of 2×10^{-6} can be obtained. Pressure of this order can be measured with the help of a Penning gauge.

Figure 1. Photograph of the assembled UHV compatible field emission set-up.

Figure 2. Top view of the field-emission set up

The sample can be mounted on the cathode plate with silver paste. Electrical circuitry was designed in order to apply field to anode and cathode plates. The anode plate was connected to the positive terminal of the high voltage DC power supply unit (model no H5K02N of Aplab of 5 k V rating) through Keithley meter. A high resistance of 7.7 MΩ was connected in series with the power supply for limiting the current and to avoid accidental damage of power supply and current meter. The cathode electrode was grounded to the power supply and grounded to earth through the chamber body and mount.

Figure 3. The digitally controlled cathode movement set up below the chamber.

Figure 4: The diode assembly seen from top with the chamber cover open.

The diode assembly from top, with the chamber cover open is shown in Figure 4 while the schematic of the complete diode type field-emission measurement set-up is shown in Figure 5. A high-resolution CMOS camera (ARTCAM-200MI) is assembled on top of the glass view port and interfaced with PC with high speed transfer via USB 2.0 interface for taking the in-situ pictures of emission from CNT films. For the I-V characteristic measurement, the polished SS plate was kept on the anode and for emission pattern imaging, a conducting fluorescent screen is placed over the anode.

Table 1. Details of samples prepared by varying the gas flow ratio and time of deposition

Sample	Gas flow ratio C_2H_2:H_2(in sccm)	Deposition time
A	20:70	2 min
B	15:75	2 min
C	20:70	1 min
D	15:75	1 min

2.2. Growth of carbon nanotube films

CNT films were grown by tubular MPECVD system. Iron films of thickness ~ 5 nm were deposited on p-Si (100) substrates by thermal evaporation technique. Growth of these films includes the following steps: (1) pretreatment of catalyst coated substrates in Ar and H_2 plasma followed by (2) introduction of acetylene (C_2H_2) for film deposition. The microwave power, substrate, heating pressure, deposition pressure and catalyst pretreatment time were kept constant as 570 W, 2.4 Torr, 5 Torr and 15 min. respectively while the flow rates of H_2 and C_2H_2 and the time of deposition were varied to study the effect of varying parameters on the morphology and structural properties of deposited films. The details of various samples prepared are given in Table 1.

Surface morphology of the films was investigated by scanning electron microscopy (SEM) (ZEISS EVO 50) operating at 20 k V accelerating voltage. Microstructures of CNTs were examined by transmission electron microscopy (TEM) (Philips CM12) operating at 100 kV

2.3. Field Emission Measurements

The electron field emission measurements were carried out for various samples to study the effect of structure and surface morphology of CNT films on their field emission properties. For this, the sample (to be studied) was mounted over the cathode with silver paste. The distance between the cathode and the anode was digitally adjusted to a value of 250 µm. The base pressure of the chamber achieved by a rotary and turbo molecular pump combination is ~ 1×10^{-6} torr. The circuit for I-V measurement was then assembled and variable positive voltage starting from 350 V up to 2700 V (varying in steps of 50 V) was applied to the anode and current was measured with Keithley digital multimeter.

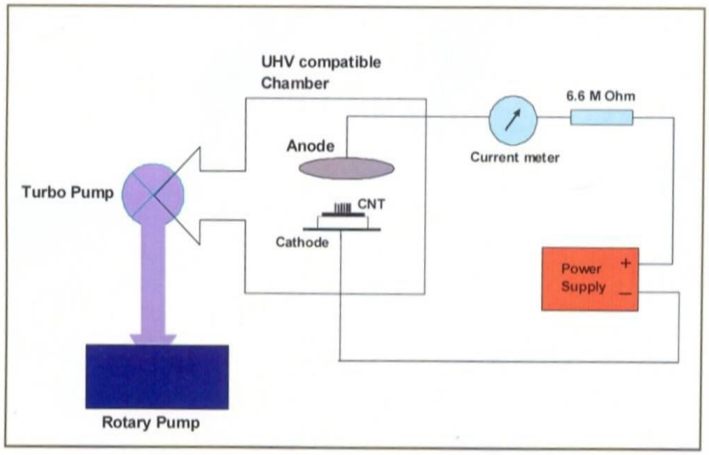

Figure 5. Schematic of the diode type field-emission measurement set-up.

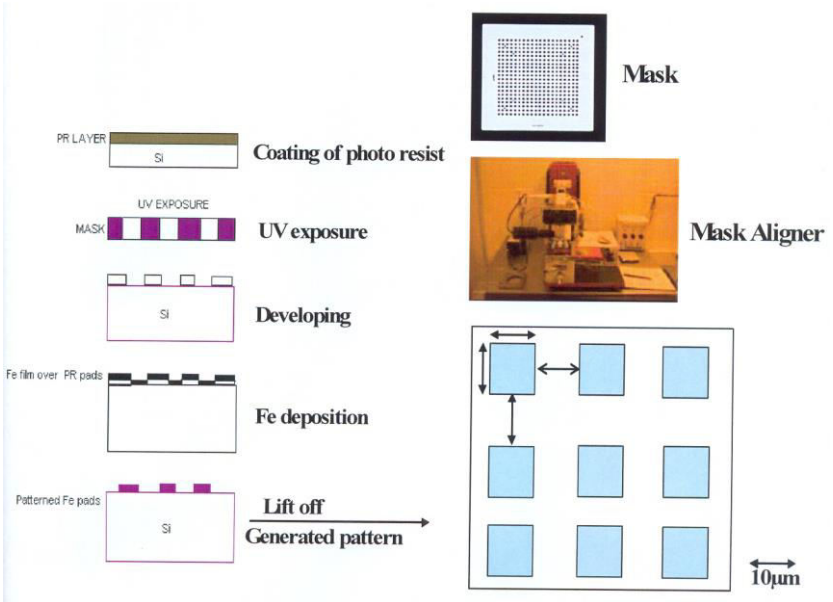

Figure 6. Schematic of photolithography process for generating the Fe deposited patterned structure on silicon wafer

Two sets of reading were taken for each sample with increasing and decreasing voltages and averaged out. The effective voltage applied was obtained by subtracting the voltage drop across the 7.7 M ohm resistance from the applied voltage. The electric field (E) was found by dividing the V_{eff} by the distance between the cathode and anode. The current density (J) was calculated by dividing the current obtained with the area of the sample covered by carbon film. The current density vs electric field was plotted from which the turn-on field was determined. From the F-N plot, the geometrical field enhancement factor was calculated.

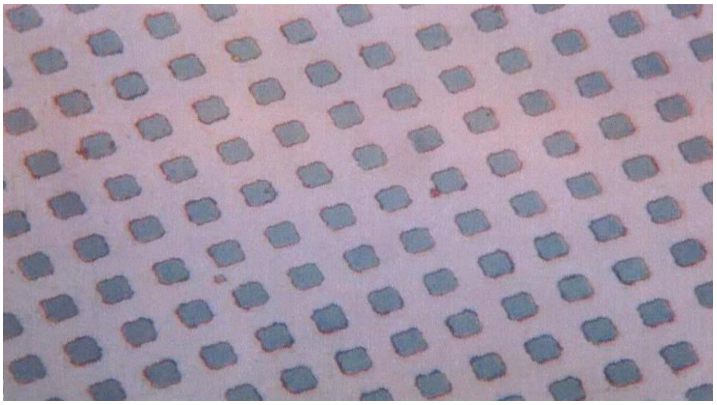

Figure 7. The 10 μm x 10 μm Fe pads seen under an optical microscope.

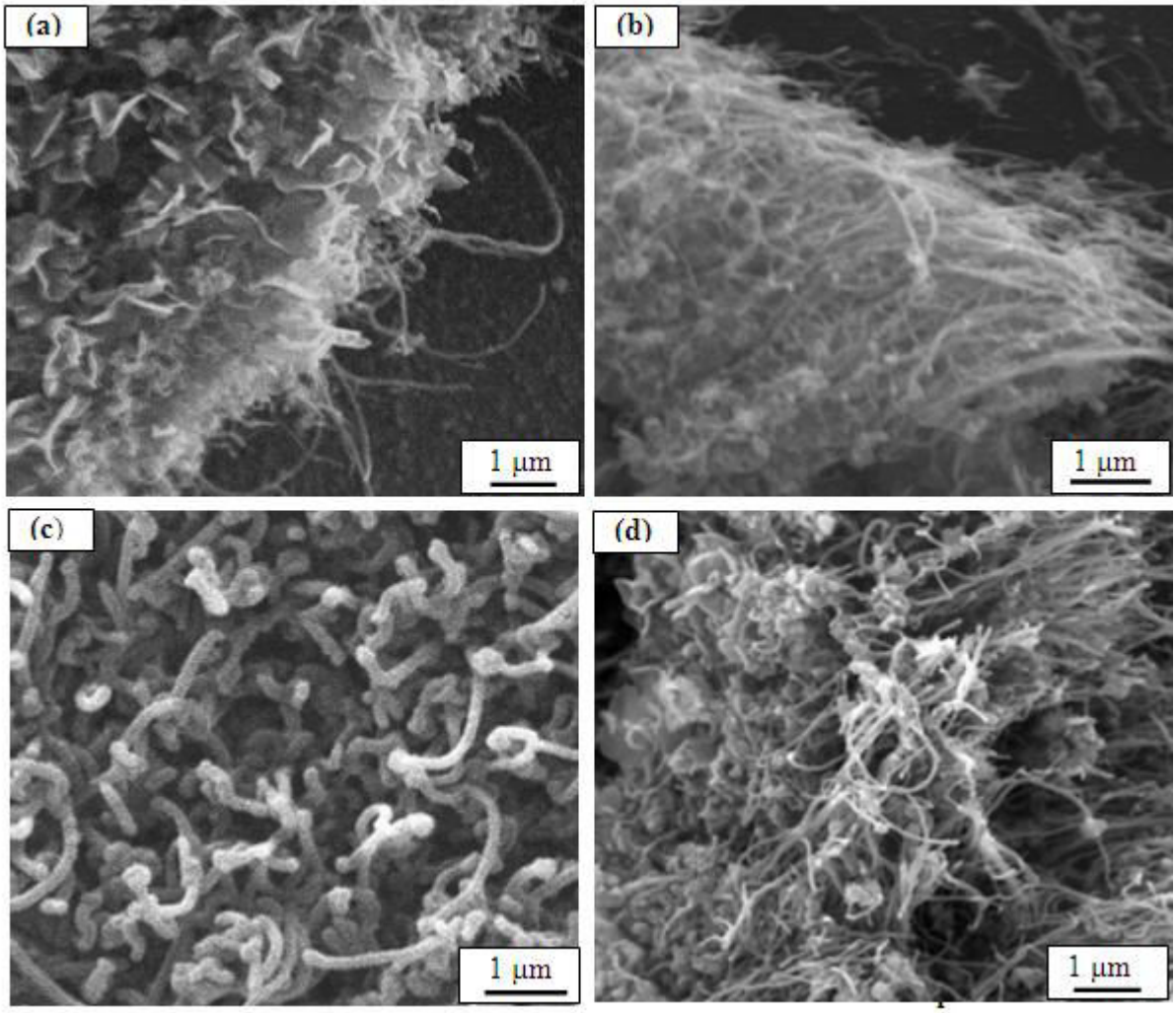

Figure 6. SEM micrographs of samples A-D

2.4. Growth of CNTs on patterned substrate

The photolithography process was employed to generate a pattern on silicon wafer at Solid State Physics Laboratory (SSPL), New Delhi. A square pattern of size 10 μm x 10 μm of Fe pads with inter separation of 10 μm was deposited on p-Si (100) wafer. The process involved preparation of mask of 10 μm x 10 μm size by a laser designator. A photoresist was coated on the substrate and exposed to UV light through the mask and developed with the standard alkaline developer solution. Further Fe of 5 nm thickness was coated on the generated pattern by DC sputtering and finally lift-off of the photoresist layer gave rise to the desired structure. The details of the process are depicted schematically in Figure 6. The Fe pads were seen under an optical microscope. Figure 7 shows the patterned wafer image. CNT growth was carried out on this substrate for a duration of 2 min. The flow ratios of H_2 and C_2H_2 were kept as 15 sccm and 90 sccm respectively. The other parameters of MPECVD process were kept same as given in 3.2. This sample was named as sample E.

3. Results and Discussion

3.1. Growth and Morphology

The continuous Fe films were converted into quasi-spherical nanoparticles of size varying from 20-100 nm after plasma pretreatment (not shown here). Figure 8 shows the SEM micrographs of samples A-D. All the samples were observed to have dense growth of one-dimensional structures. However, in sample A, rose petal like structures were observed on the top surface. These one-dimensional structures were confirmed to be carbon nanotubes by TEM and HRTEM studies. The petals like structures are two-dimensional

graphitic nanoflakes. As the H_2 flow ratio was increased to 15:75 (sample B), carbon nanoflakes were rarely observed over CNTs. This may be due to increased etching with the increased H_2 flow ratio. The time of deposition also influences the structure and morphology of deposited films as purely one-dimensional structures have been observed in samples C and D with reduced (1 min) time of deposition. This is in accordance with the observation by S.K. Srivastava et al [16] who reported the deactivation of catalyst nanoparticles due to deposition of excess carbon over their surface as the time of deposition increases. The SEM micrograph of sample E (Figure 9) shows the growth of CNTs only on the areas where catalyst is present and absence of growth at bare silicon substrate.

3.2. Microstructure of CNTs

Figure 10 shows the TEM micrographs of samples A-D. The inset of Figure 10 (a) shows the TEM micrograph of a single CNT in sample A under higher magnification. The length of CNTs in sample A was found to vary from 2 – 4.5 μm. The outer and inner diameters of a single CNT were found to be ~ 20 nm and 10 nm respectively. The outer diameter of CNTs in sample B (Figure 10(b)) varied in the range 20-30 nm while the inner diameter varied from 10 nm to 15 nm. The internal structure of carbon nanotubes consisted of many hollow compartments of nearly equal length, resembling the structure of a bamboo-shoot hence the name bamboo-shoot CNTs. Catalytic particles are observed at the ends of CNT indicating the presence of 'base growth mode' as no catalytic particles were observed at the top of CNTs in the SEM images. From the TEM micrograph of sample C (Figure 10 (c)) the outer diameter of CNT is ~ 20 nm while the inner diameter is ~ 10 nm. Compartments are seen along the length of CNT however these are not equal in size. The outer diameter of CNTs was found to vary in the range 10-25 nm while inner diameter ~ 10 nm in sample D. Thus, no large variation in diameter of CNTs is observed on varying the gas flow ratio. Also, some catalyst particles are observed inside the CNTs as well.

The TEM micrograph of the sample E shown in Figure 11 shows CNTs of length ~ 10 μm and diameter ~ 30 nm. Thus, a considerable increase in the length of CNTs was observed in case of patterned substrates.

3.3. Field Emission Results

The emission current density (J) versus applied electric field (E) plots samples A-D are given in Figure 12 (a). Defining the threshold field as the field corresponding to 100 μ A/ cm^2, we have observed E_T = 2.87, 2.45, 1.95 and 1.84 V/ μm for samples A-D respectively. The ln (J/E^2) vs. 1/E plots for samples A-D are given in Figure 12(b). A straight line with a negative slope indicates the validity of Fowler – Nordheim model. The slope of this plot is - ($b \varphi^{3/2}$) /β. Taking φ = 5 e V, the field-enhancement factor (β) was calculated for all the samples. These were found to be 4986, 7170, 7186, and 9267 for samples A-D respectively. The lower threshold field for sample B (as compared to sample A) was due to lesser surface coverage of one-dimensional film by carbon nanoflakes. The sharp tips of CNTs (having very large aspect ratio) give rise to large field enhancement and correspondingly greater electron emission (i.e. larger current density at a particular electric field) as compared to other carbon nanostructures.

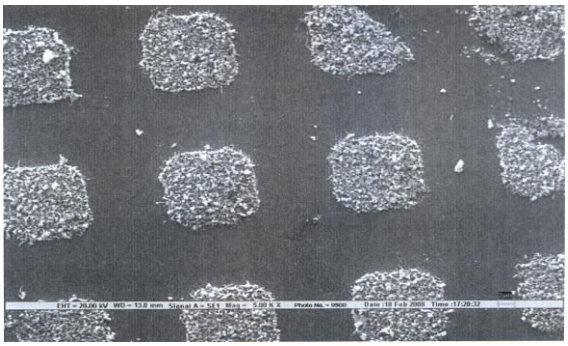

Figure 9. CNTs grown on patterned silicon substrate, each pad (square area of CNTs) is of dimension 10 μm x 10 μm.

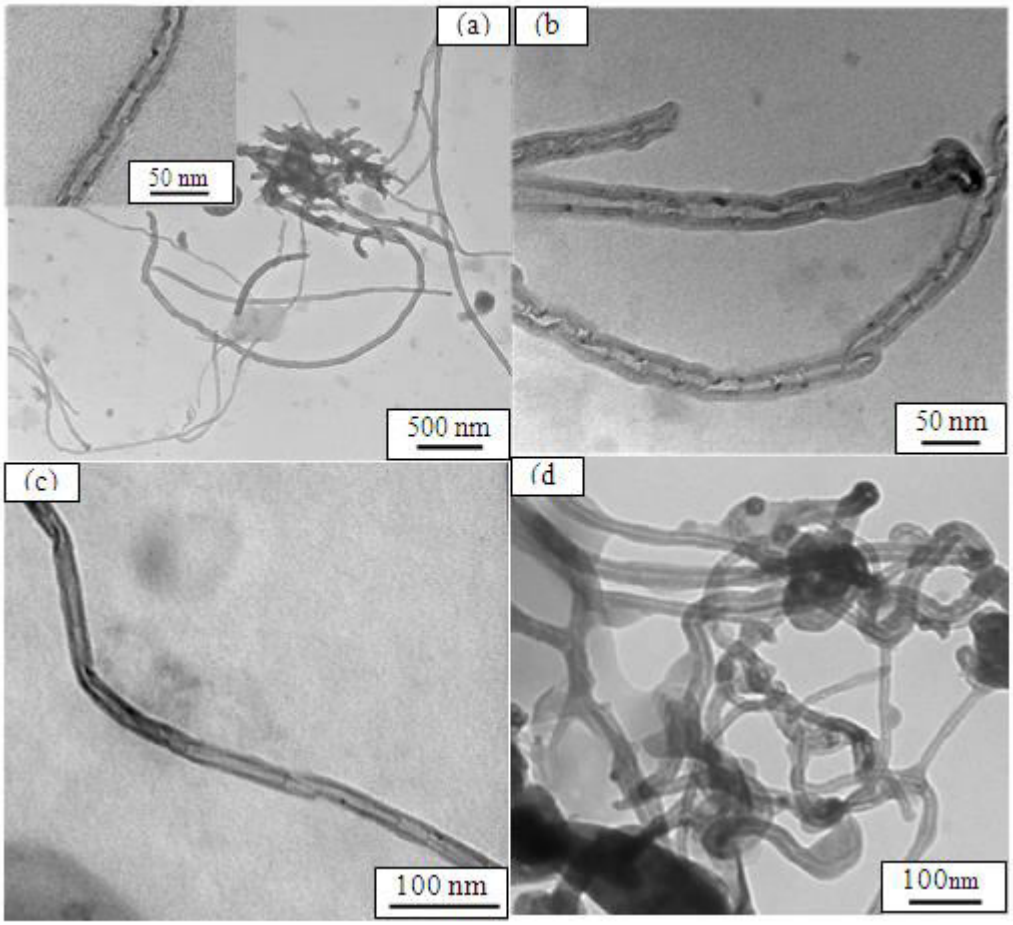

Figure 10. TEM micrographs of samples A-D

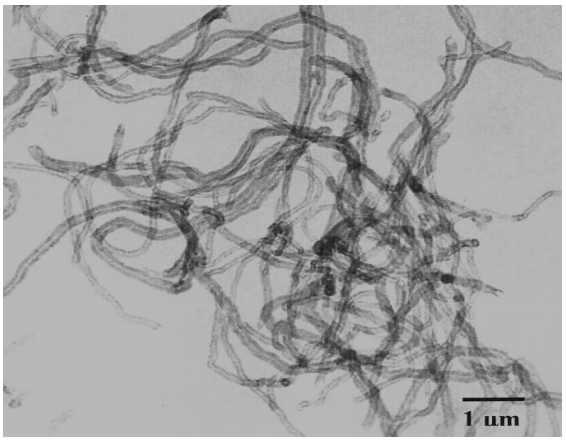

Figure 11. TEM micrographs of sample E.

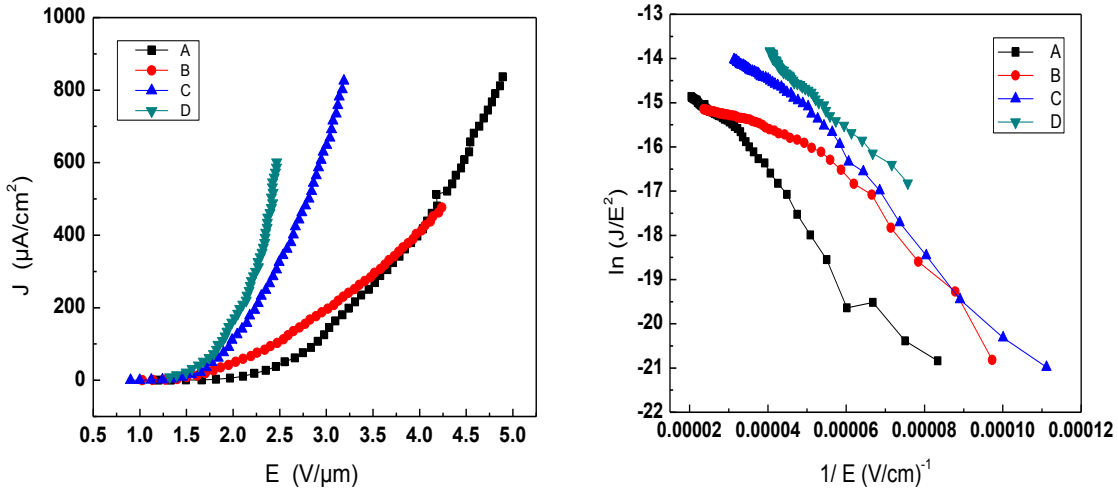

Figure 12. (a) Emission current density versus applied electric field of nanostructured carbon films. (b) Fowler-Nordheim plots of samples A-D.

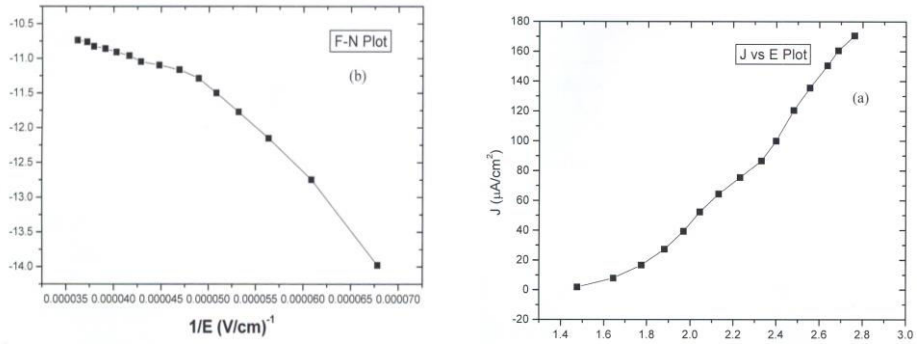

Figure 13 (a) Emission current density versus applied electric field for sample E.

(b) The corresponding F-N plot.

Although carbon nanoflakes (having sharp edges normal to the substrate) are supposed to exhibit good field emission, yet low aspect ratio and lesser crystallinity of the film (having carbon nanoflakes) degrade their emission properties. The reduction in threshold field for samples C (as compared to samples A and B) was due to the purely one-dimensional character of the film. Absence of carbon nanoflakes leads to the direct exposure of CNT tips to the applied field and a larger number of electrons are emitted due to higher geometrical field enhancement obtained. Better vertical alignment of carbon nanotubes to the substrate in case of sample D could be the reason for lower threshold field and higher field enhancement factor as compared to sample C where most of the CNT tips were bent.

The J vs E and F-N plots for sample E are given in Figure 13. The threshold field and the field enhancement factor were found to be ~ 2.40 V/ μm and 6928 respectively.

4. Conclusions

A new UHV compatible field emission set up has been described in this work. This system was indigenously designed and integrated and made operational. This field emission set-up has several salient features including the UHV compatibility, achievability of high order of vacuum, in situ adjustment of distance between the electrodes, and capturing of field emission images by the high precision CMOS camera. The field emission properties of CNT films synthesized by MPECVD method have been studied using this field emission set up. CNTs have also been successfully grown over the substrates having photo lithographically patterned catalyst film.

5. Acknowledgements

The authors are thankful to SSPL (Solid State Physical Laboratory) for carrying out photolithography processes.

6. References

[1] S. Iijima, Nature, 354 (1991) 56.

[2] M.F. Yu, B.S. Files, S. Arepalli, R.S. Ruoff, Phy. Rev. Lett. 84 (2000) 5552.

[3] V.N. Popov, Materials Science and Engg. R 43 (2004) 61-102.

[4] P.M. Ajayan, Otto Z. Zhou, Topics Appl. Phys. 80 (2001) 391-425.

[5] T. W. Ebbesen and P. M. Ajayan, Nature, 358 (1992) 220.

[6] Y. Ando, X. Zhao and M. Ohkohchi, Carbon, 35 (1997) 153.

[7] A. Thess, R. Lee, P. Nikolaev, H. Dai, P. Petit, J.Robert, C.Xu, Y.H. Lee, S.G. Kim, A.G. Rinzler, D.T. Colbert, R.E. Smalley, Science 273 (1996) 483.

[8] A.M. Cassell, J.A. Raymakers, J. Kong, and H.J. Dai, J. Phys. Chem. B 103 (1999) 6484.

[9] A.V. Eletskii, Physics - Uspekhi 45 (4) (2002) 369-402.

[10] Yuan Cheng, Otto Zhou, C.R. Physique 4 (2003)

[11] Q.H. Wang, A.A. Setlur, J.M. Lauerhass, J.Y. Dai, E.W. Seelig, R.P.H. Chang, Appl. Phys. Lett. 72 (22) (1998) 2912.

[12] Q.H. Wang, M. Yang, R.P.H. Chang, Appl. Phys. Lett. 78 (9) (2001) 1294.

[13] F. Ito, Y. Tomihari, Y. Okada, K. Konama, A. Okamoto, IEEE Electron Device Letters 22 (9) (2001) 426-428.

[14] N.S. Lee, D. S. Chung, I.T. Han, J.H. Kang, Y.S. Choi, H.Y. Kim, S.H. Park, J.M. Kim, Diamond and Related Materials 10 (2001) 265-270.

[15] H.Y. Choi, J.U. Kim, C.J. Lee, Acta Physica Polonica A 115 (2009) 1078-1080.

[16] S.K. Srivastava, A.K. Shukla, V. D. Vankar, V. Kumar, Thin Solid Films, 492 (2005) 124-130.

[17] S.K. Srivastava, V. D. Vankar, V. Kumar, Thin Solid Films, 515 (2006) 1552-1560.

[18] J.M. Bonard, K. Kern, Appl. Phys. Lett., 76 (2000) 2